Science Advances
AAAS

advances.sciencemag.org/cgi/content/full/6/46/eaba9543/DC1

Supplementary Materials for

Ultrastrong lightweight compositionally complex steels via dual-nanoprecipitation

Zhangwei Wang*, Wenjun Lu*, Huan Zhao, Christian H. Liebscher, Junyang He, Dirk Ponge, Dierk Raabe, Zhiming Li*

*Corresponding author. Email: zh.wang@mpie.de (Z.W.); w.lu@mpie.de (W.L.); lizhiming@csu.edu.cn (Z.L.)

Published 13 November 2020, *Sci. Adv.* **6**, eaba9543 (2020)
DOI: 10.1126/sciadv.aba9543

The PDF file includes:

Other Supplementary Material for this manuscript includes the following:

(available at advances.sciencemag.org/cgi/content/full/6/46/eaba9543/DC1)

Table S1. Chemical composition of the model CCS according to wet-chemical analysis.

	Fe	Mn	Al	Ni	C
wt. %	55.23	29.6	8.75	5.22	1.20
at. %	48.34	26.38	15.89	4.49	4.90

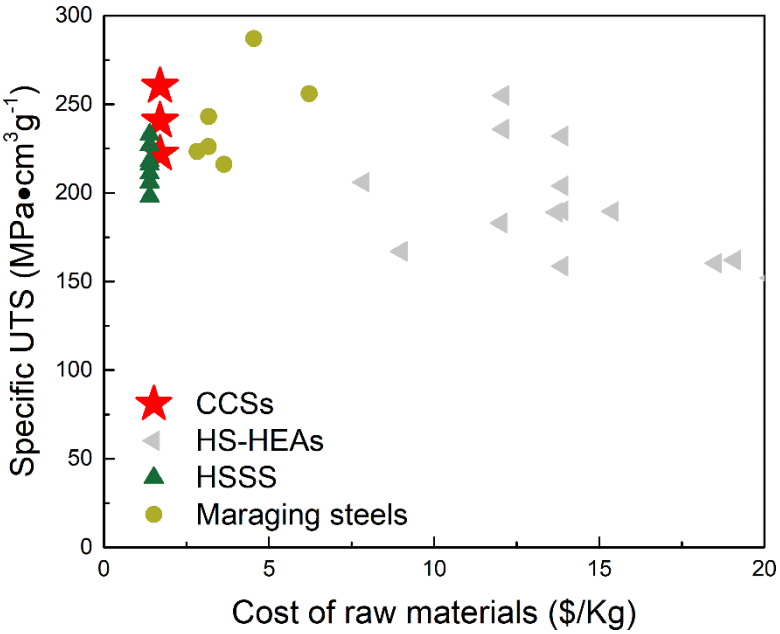

Fig. S1. Cost of raw materials versus specific UTS. Our CCSs, high-strength (HS) HEAs (*21*, *24-33*), HSSS (*6*, *7*), and maraging steels (*22*, *23*) are shown for comparison.

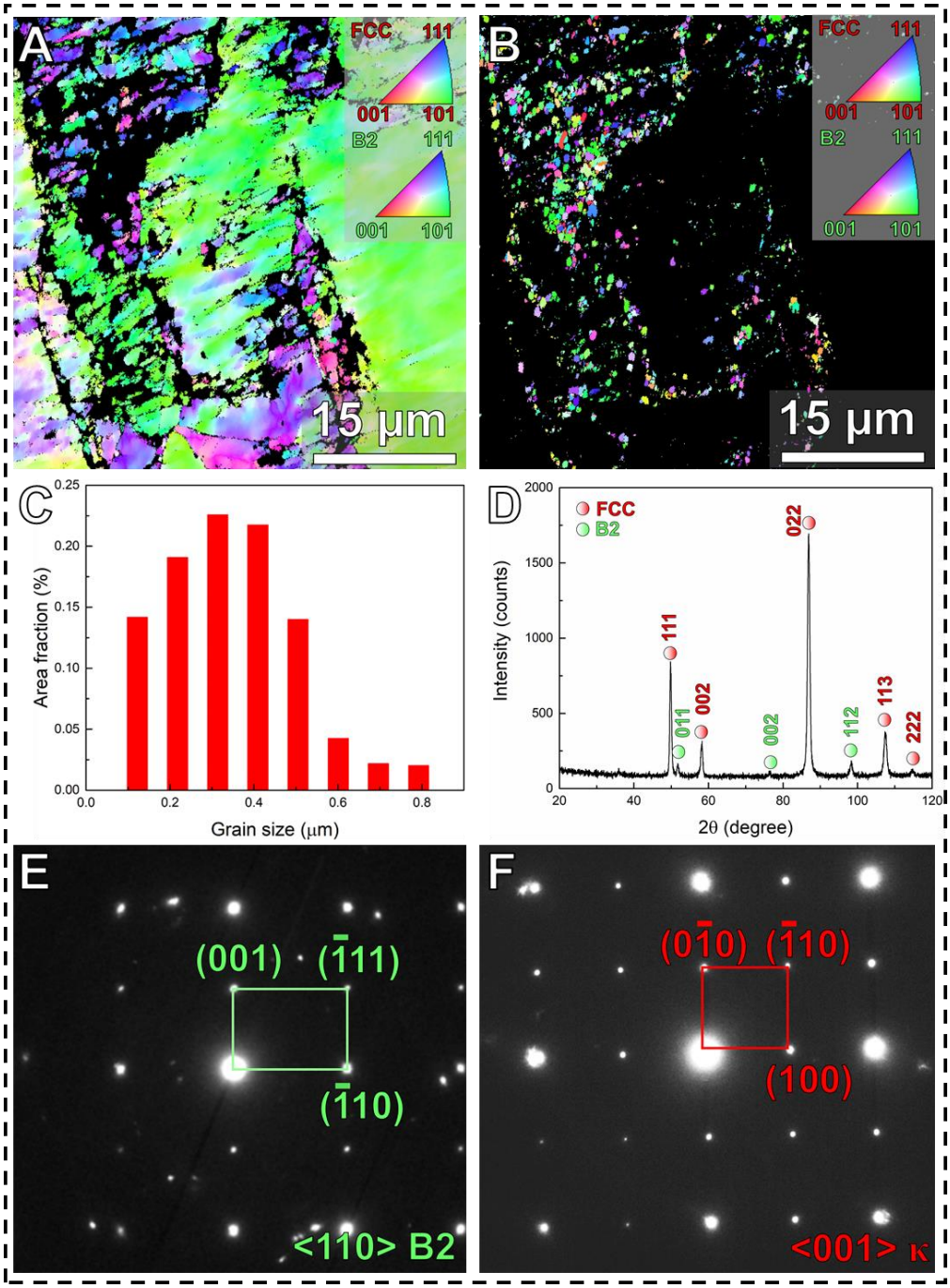

Fig. S2. Microstructures of the model CCS annealed at 800 °C. IPF maps showing the (**A**) non-recrystallized area and (**B**) recrystallized area. (**C**) The grain size distribution in the recrystallized area. The area fraction of the recrystallized area is 8 %, and the corresponding average grain size is 0.35 μm in this area. **(D)** XRD pattern. The peaks of FCC structure contain the information from both austenite matrix and κ-carbides, since the XRD analysis cannot differentiate between them. SAED patterns of B2 (inset in Figure 1D) and κ-carbide (inset in Figure 1G) are indexed in (**E**) and (**F**), respectively. Due to the very small size of B2 particle, austenite matrix was also included when performing the SAED, causing the appearance of satellite spots in (E).

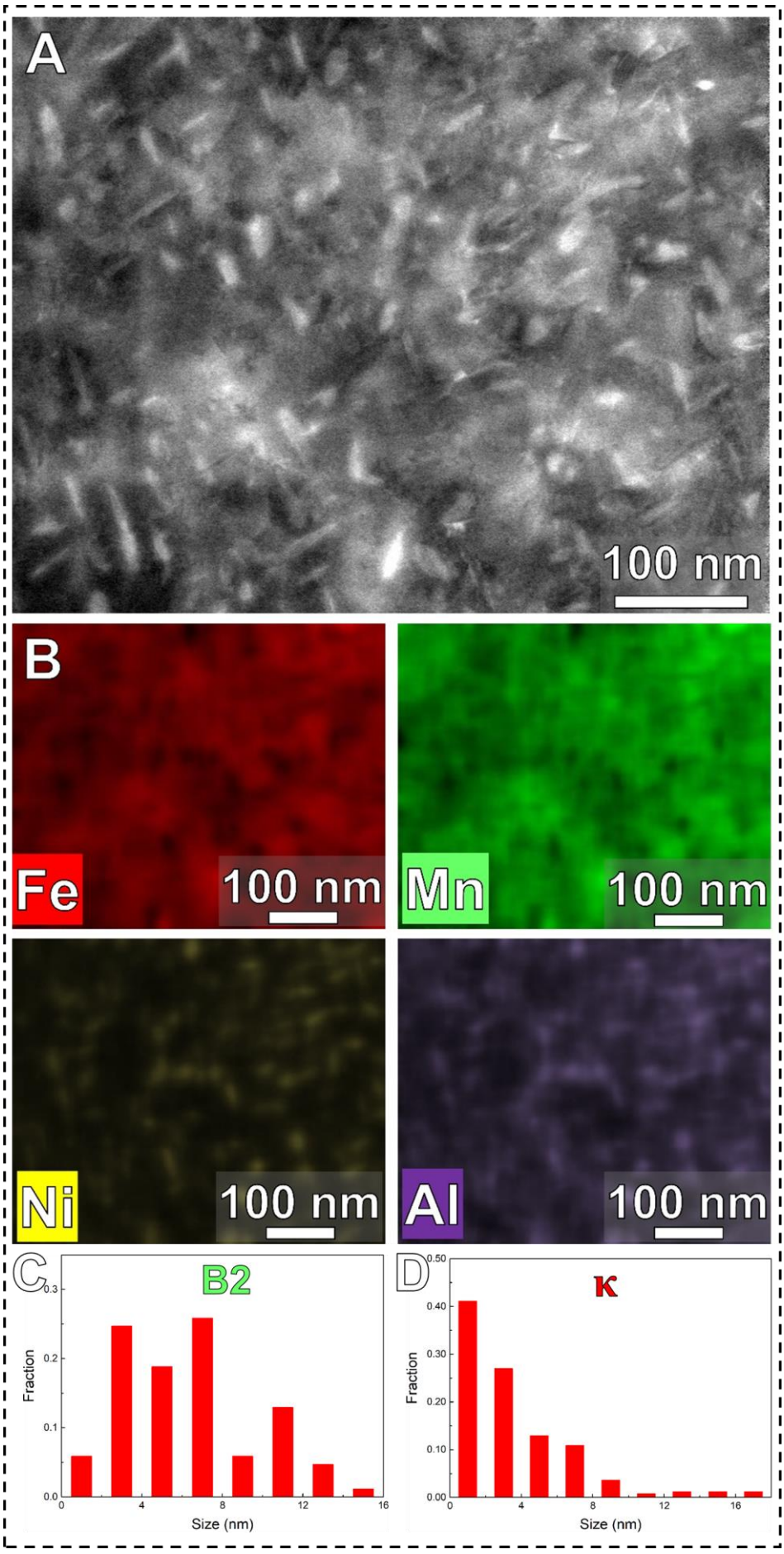
A
100 nm
B
Fe
100 nm
Mn
100 nm
Ni
100 nm
Al
100 nm
C
B2
Fraction
Size (nm)
D
κ
Fraction
Size (nm)

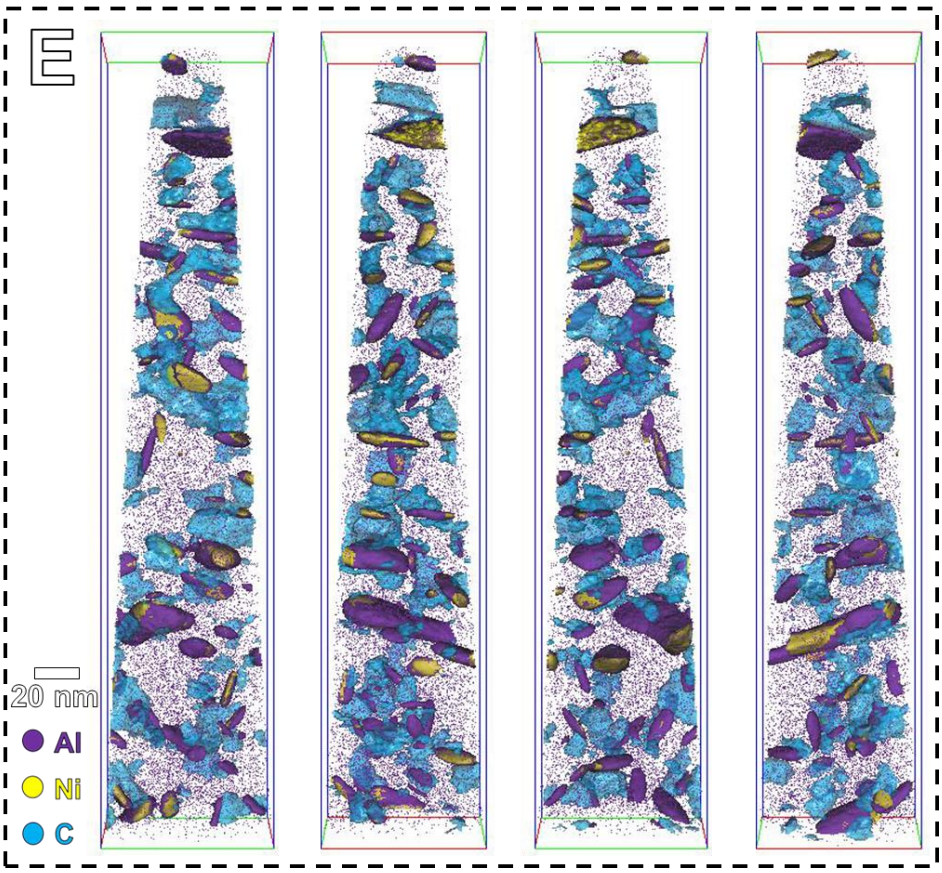

Fig. S3. Characterization of dual-nanoprecipitation in the model CCS annealed at 800 °C. (**A**) HAADF-STEM image. (**B**) EDS maps. The size distributions of very fine **(C)** B2 particles and **(D)** κ-carbides. The average sizes of B2 and κ-carbide are ~6 nm and ~4 nm, respectively, which have been determined by APT analysis. (**E**) Reconstructed maps from atom probe tomography probing of a typical tip shown in Fig. 2E, viewed from four different directions (highlighted by iso-composition surfaces of 30 at. % Ni, 30 at. % Al, and 10 at. % C), which clearly reveal the co-precipitation of B2 and κ-carbide with adjacent positions, referred to here as backpack topology.

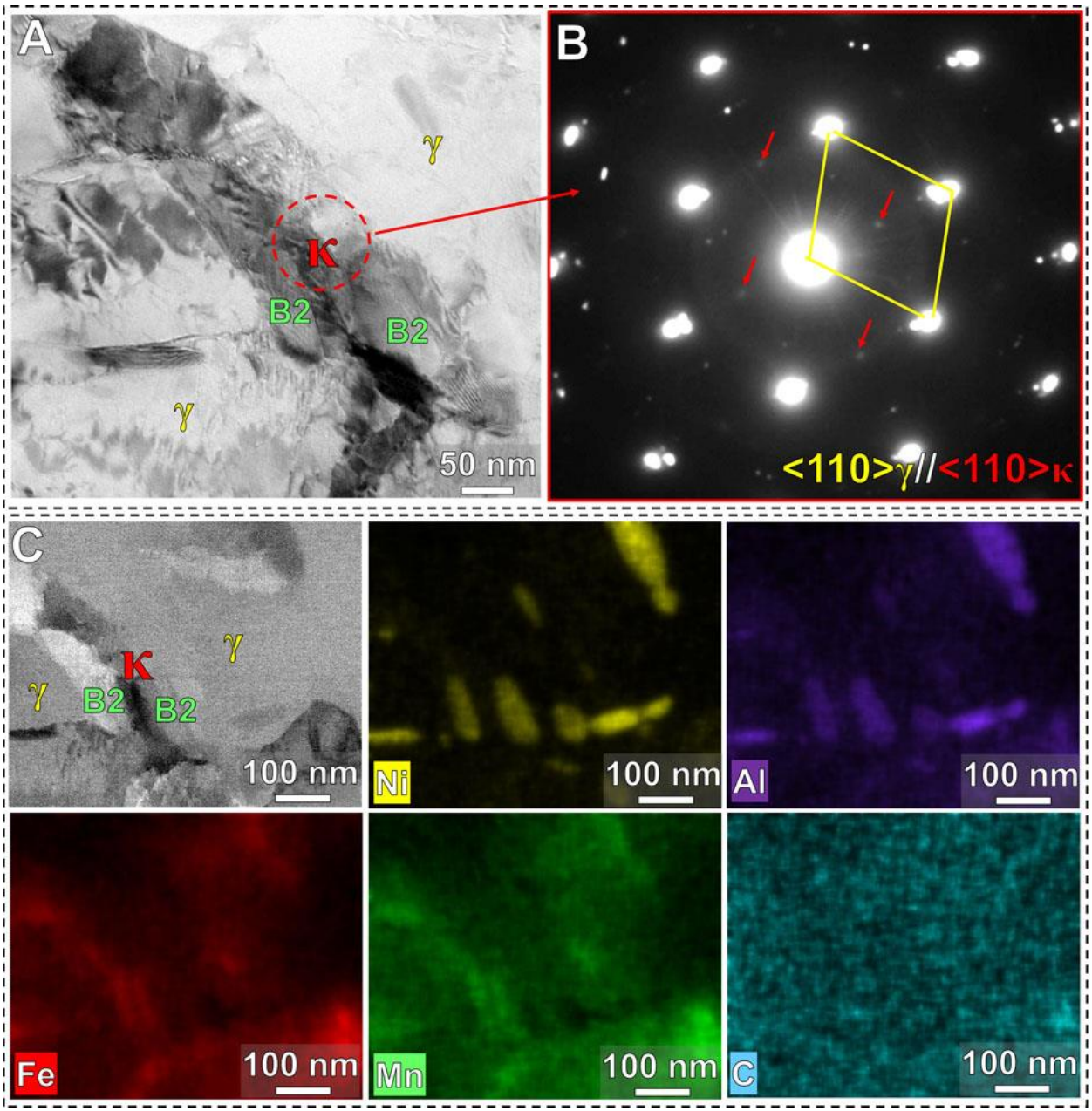

Fig. S4. Dual-nanoprecipitation in the model CCS annealed at 900 °C. (**A**) Bright-field TEM image and (**B**) SAED pattern. The formation of κ-carbide is revealed by the SAED pattern in (B), and the existence of B2 phase is identified by the EDS maps in (**C**). The co-precipitation of κ-carbide and B2 phase still exists even when annealed at higher temperatures such as 900°C.

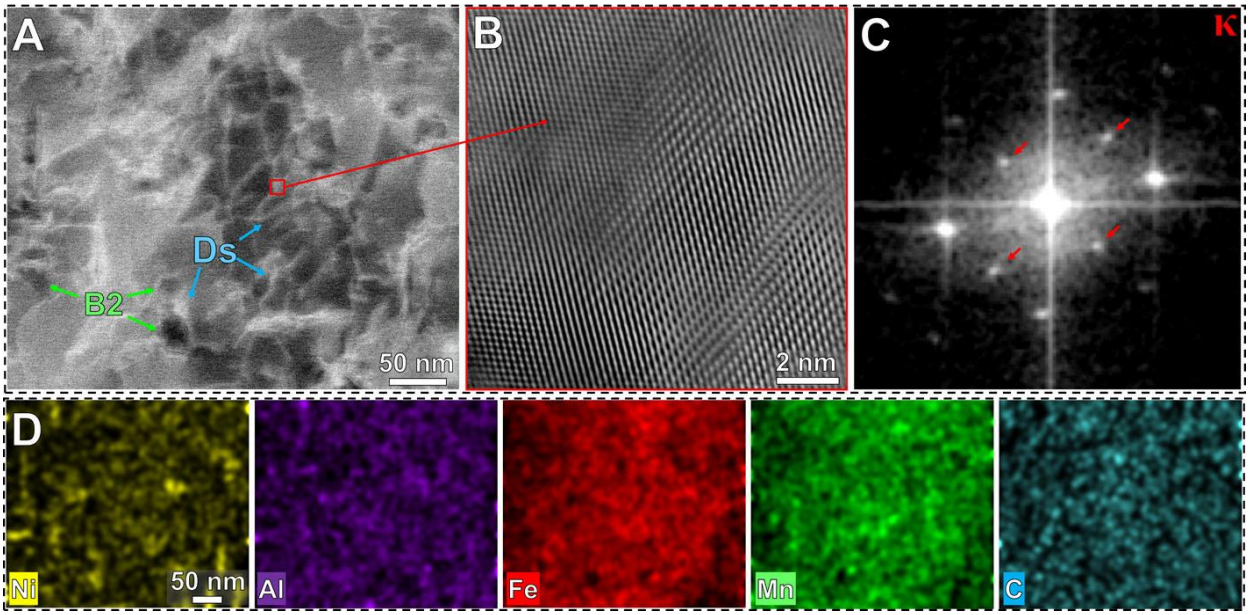

Fig. S5. Deformation microstructures of the model CCS annealed at 800 °C at 7 % strain. (**A**) LAADF-STEM image showing the dislocations (Ds, in bright contrast). (**B**) HR HAADF-STEM image of the marked region in (A). (**C**) The corresponding FFT pattern for (B) showing the existence of κ-carbides. (**D**) EDS maps for (A) showing the existence of B2 particles. Much more dislocations were seen at a higher strain. Again, B2 particles pinned the dislocation movements, while κ-carbides were cut through by dislocations.

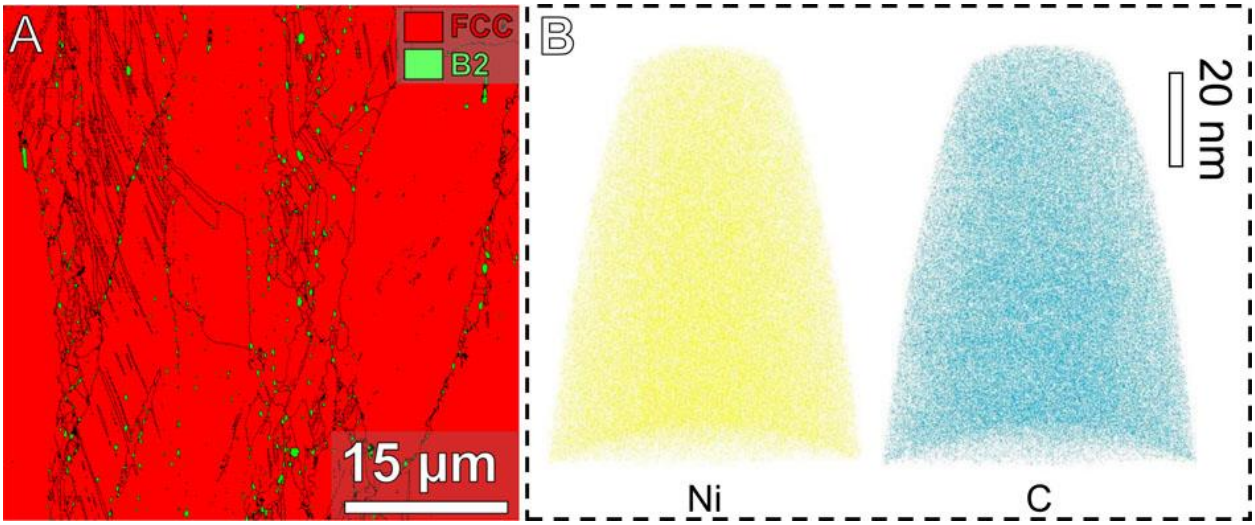

Fig. S6. Microstructure and nanoscale elemental distribution of the hot-rolled CCS. (**A**) The EBSD phase map shows that the B2 particles were formed during hot-rolling. The black lines in (A) represent the high angle grain boundaries. (**B**) Reconstructed atomic maps of Ni and C based on APT analysis show that the very fine nano-precipitation did not occur during the hot-rolling process.

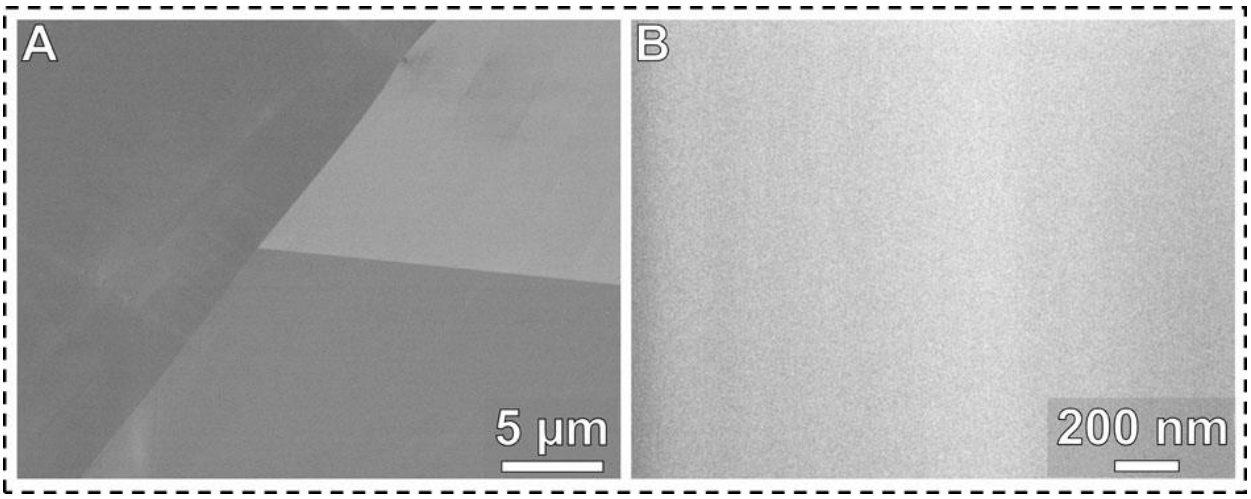

Fig. S7. Microstructures of the model CCS homogenized at 1200 °C for 1 h. (**A**) BSE image and (**B**) HAADF-STEM image show that nearly all precipitates dissolve into the austenite matrix after homogenization.

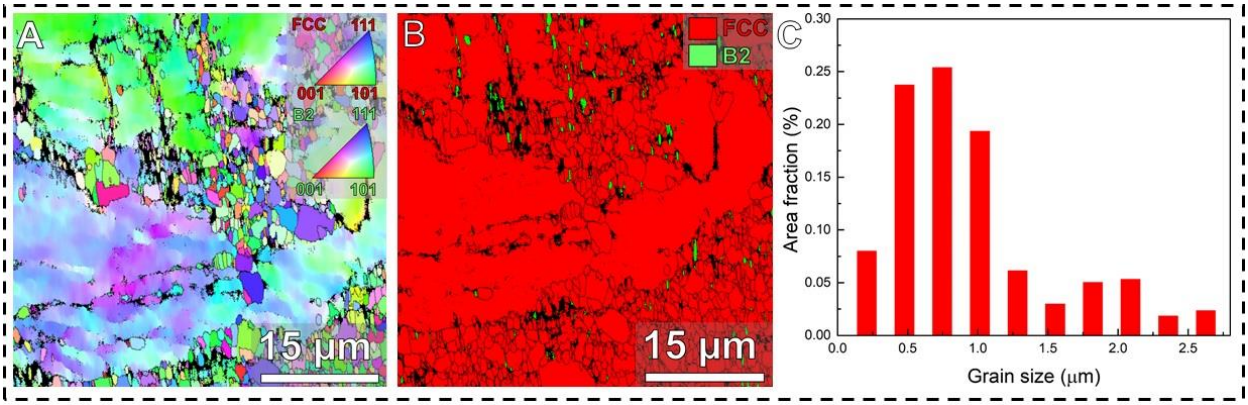

Fig. S8. EBSD maps of the model CCS annealed at 850 °C. (**A**) IPF map and (**B**) phase map, and (**C**) the grain size distribution in the recrystallized area. The black lines in (B) represent the high angle grain boundaries. The area fraction of the recrystallized area is 28 %, and the corresponding average grain size is 1.0 μm in this area.

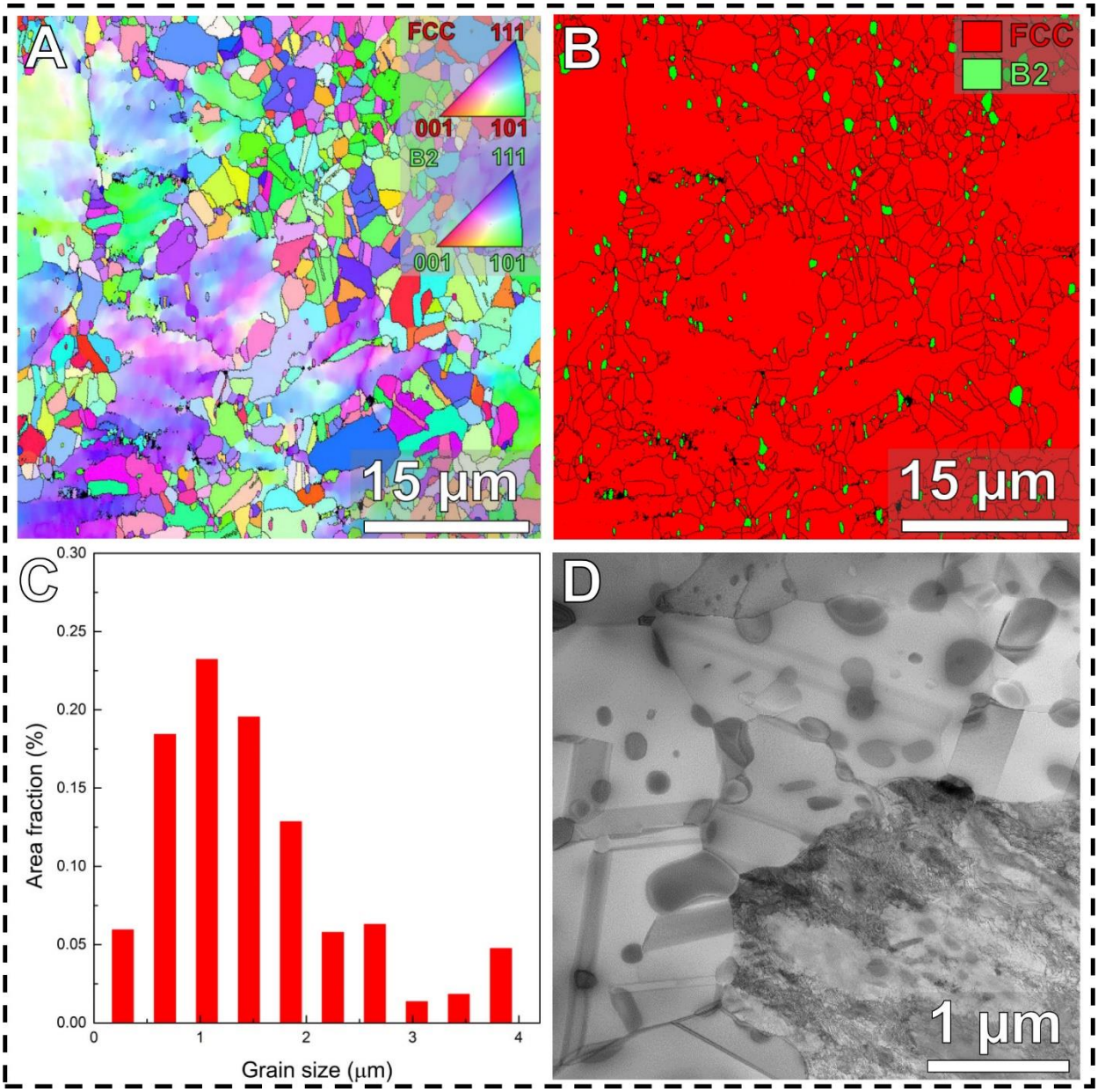

Fig. S9. EBSD maps and STEM image of the model CCS annealed at 900 °C. (**A**) IPF map, (**B**) phase map, (**C**) the grain size distribution in the recrystallized area, and (**D**) bright-field STEM image. The black lines in (A) and (B) represent the high angle grain boundaries. The area fraction of the recrystallized area is 57 %, and the corresponding average grain size is 1.5 μm in this area.

Movie S1. 3D exhibition of APT dataset in Fig. 2E showing the dual-nanoprecipitation of κ-carbides and B2 particles.